JCTC Journal of Chemical Theory and Computation

Insight into the Role of Mg^{2+} in Hammerhead Ribozyme Catalysis from X-ray Crystallography and Molecular Dynamics Simulation

Tai-Sung Lee,*,†,‡ Carlos Silva-López,‡ Monika Martick,§ William G. Scott,§ and Darrin M. York*,‡

Consortium for Bioinformatics and Computational Biology and Department of Chemistry, University of Minnesota, 207 Pleasant St. SE, Minneapolis, Minnesota 55455, and Department of Chemistry and Biochemistry and the Center for the Molecular Biology of RNA, Sinsheimer Laboratories, University of California at Santa Cruz, Santa Cruz, California 95064

Received October 25, 2006

Abstract: Results of a series of 12 ns molecular dynamics (MD) simulations of the reactant state (with and without a Mg^{2+} ion) and early and late transition state mimics are presented based on a recently reported crystal structure of a full-length hammerhead RNA. The simulation results support a catalytically active conformation with a Mg^{2+} ion bridging the A9 and scissile phosphates. In the reactant state, the Mg^{2+} spends significant time closely associated with the 2′OH of G8 but remains fairly distant from the leaving group $O_{5'}$ position. In the early TS mimic simulation, where the nucleophilic $O_{2'}$ and leaving group $O_{5'}$ are equidistant from the phosphorus, the Mg^{2+} ion remains tightly coordinated to the 2′OH of G8 but is positioned closer to the $O_{5'}$ leaving group, stabilizing the accumulating charge. In the late TS mimic simulation, the coordination around the bridging Mg^{2+} ion undergoes a transition whereby the coordination with the 2′OH of G8 is replaced by the leaving group $O_{5'}$ that has developed significant charge. At the same time, the 2′OH of G8 forms a hydrogen bond with the leaving group $O_{5'}$ and is positioned to act as a general acid catalyst. This work represents the first reported simulations of the full-length hammerhead structure and TS mimics and provides direct evidence for the possible role of a bridging Mg^{2+} ion in catalysis that is consistent with both crystallographic and biochemical data.

The hammerhead ribozyme[1] is an archetype system to study RNA catalysis.[2,3] A detailed understanding of the hammerhead mechanism provides insight into the inner workings of more complex cellular catalytic RNA machinery such as the ribosome and ultimately may aid the rational design of new medical therapies[4] and biotechnology.[5,6]

Despite a tremendous amount of experimental and theoretical effort,[1,2,7,8] the details of the hammerhead ribozyme mechanism have been elusive. In particular, one of the main puzzles involves the apparent inconsistency between the interpretation of thio effect experiments[9,10] and mutational data[8] with available crystallographic structural information of the minimal hammerhead sequence.[11−13] Results from the biochemical experiments suggest that a pH-dependent conformational change, inconsistent with crystallographic data,[11−13] must precede or be concomitant with the catalytic chemical step. This includes a possible metal ion bridge between the A9 and scissile phosphates that in previous crystal structures were ∼20 Å apart. Moreover, the function of the 2′OH group of G8 remains unclear.

Very recently, the crystallographic structure of a full length hammerhead sequence has been determined at 2.2 Å resolution.[14] The naturally occurring full-length hammerhead sequence exhibits enhanced catalytic activity and a different metal ion requirement relative to the minimal motif.[15] The crystal structure has the A9 and scissile phosphates in close proximity, consistent with the interpretation of thio effect measurements,[9] and the 2′OH of G8 and N_1 of G12 poised to act as a general acid and base, respectively, consistent with photocrosslinking experiments[16] and mutational data.[8] However, the divalent metal ions required for catalysis were not resolved in this structure. This letter reports the first simulations of the full-length hammerhead ribozyme in the reactant, early, and late transition states along the reaction coordinate. Results support the requirement for a bridging Mg^{2+} ion between the A9 and scissile phosphates in the catalytically active conformation and provide evidence of a role of the metal ion in catalysis that is consistent with both crystallographic and biochemical data.

Simulations were performed with CHARMM[17] (version c32a1) using the all-atom nucleic acid force field[18,19] with extension to reactive intermediates (e.g., transition state mimics)[20] and TIP3P water model.[21] Simulations of the reactant state (with and without a Mg^{2+} ion) and early and late TS mimics were each performed at 298 K and 1 atm in

* Corresponding author e-mail: york@chem.umn.edu.
† Consortium for Bioinformatics and Computational Biology, University of Minnesota.
‡ Department of Chemistry, University of Minnesota.
§ University of California at Santa Cruz.

10.1021/ct6003142 CCC: $37.00
Published on Web 01/03/2007

Table 1. Key Distances (Å) in the Hammerhead Active Site[a]

	X-ray structure	reactant	reactant w/o Mg^{2+}	early-TS mimic	late-TS mimic
C1.1:O_{P2} ↔ A9:O_{P2}	4.27	3.36(49)	7.16(110)	4.00(06)	4.01(07)
Mg^{2+} ↔ G8:$O_{2'}$	3.08[b]	3.97(102)		2.24(13)	3.21(23)
Mg^{2+} ↔ C1.1:$O_{5'}$	4.04[b]	4.22(21)		3.68(35)	2.09(05)
G8:$H_{O2'}$ ↔ C1.1:$O_{5'}$		4.57(135)	7.61(81)	5.09(74)	2.36(42)
C17:$O_{2'}$ ↔ C1.1:P	3.18	3.61(23)	3.83(19)	1.88(11)	1.75(04)

[a] The simulation results were calculated over the last 10 ns with data collected every 1 ps. Shown are average values and standard deviations in the parentheses. [b] A proposed Mg^{2+} site was assumed directly between the crystallographic positions of C1.1:O_{P2} and A9:O_{P2}.

a rhombododecahedral cell (with PME[22] electrostatics) in the presence of ~10 000 water molecules and 0.14 M NaCl and carried out to 12 ns following 1 ns of solvent equilibration. In three simulations, a single Mg^{2+} ion was positioned so as to bridge the A9 and scissile phosphates that in the crystallographic structure are around 4.3 Å, which is well suited for Mg^{2+}-bridging coordination.[23] The Mg^{2+} ion is critical for stability and adopts different coordination states along the reaction coordinate, verified by preliminary QM/MM calculations (see the Supporting Information) that are supportive of a catalytic role consistent with experiments.

A stable Mg^{2+} ion bridge between the A9 and scissile phosphates is formed in the catalytically active conformation. The simulation results support a catalytic role for a Mg^{2+} ion bridging the A9 and scissile phosphates. In the simulations with a bridging Mg^{2+} ion, the average distance between the A9 and scissile phosphates remain within the crystallographic value of 4.3 Å, whereas in the absence of Mg^{2+} this key contact between stems I and II drifts to over 7 Å (Table 1). In the reactant state, the Mg^{2+} coordination between the C1.1 and A9 phosphate oxygens fluctuates between axial−axial and axial−equatorial modes, resulting in a shorter average oxygen−oxygen distance than that observed in the X-ray structure. This may suggest that in the reactant state the preferred binding mode of Mg^{2+} is different, e.g., between A9 and N_7 of G10.1,[24,25] and that a conformational change brings Mg^{2+} into a bridging position between A9 and the scissile phosphate leading to the transition state.[9] The present simulation results suggest that the close proximity of the A9 and scissile phosphates observed in the new full-length hammerhead structure[14] can be stabilized by a Mg^{2+} ion bridge that brings together stems I and II and facilitates formation of near-attack conformations (see the Supporting Information) in a way different from previous simulations based on the minimal sequence structures.[26,27,28,29]

In the early TS, the Mg^{2+} ion is positioned to shift the pK_a of the 2′OH of G8 to act as a general acid. In the reactant state, the Mg^{2+} spends significant time closely associated with the 2′OH of G8 (Figure 1) but remains fairly distant from the leaving group $O_{5'}$ position. In the early TS mimic simulation, where the nucleophilic $O_{2'}$ and leaving group $O_{5'}$ are equidistant from the phosphorus, the Mg^{2+} ion becomes directly coordinated to the 2′OH of G8, and is positioned closer to the $O_{5'}$ leaving group. The coordination of the Mg^{2+} ion in the early TS mimic simulation is consistent with a role of shifting the pK_a of the 2′OH in G8 so as to act as a general acid (Figure 2, left).

In the late TS, the Mg^{2+} ion can act as a Lewis acid catalyst to stabilize the leaving group and is poised to assist proton transfer from the 2′OH of G8. In the late TS mimic

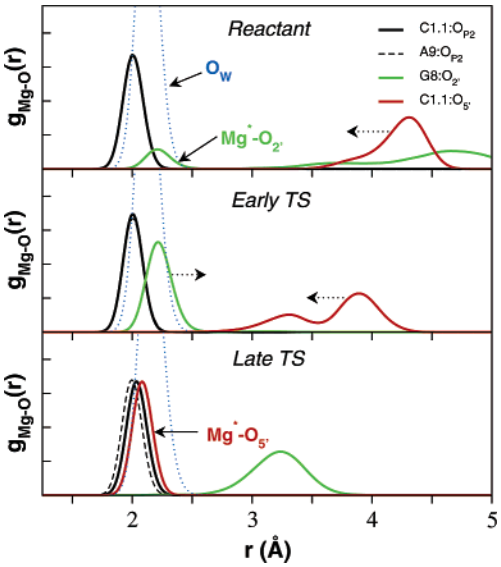

Figure 1. Radial distribution functions of key oxygens around Mg^{2+} in the active site for the reactant, early, and late TS mimic simulations.

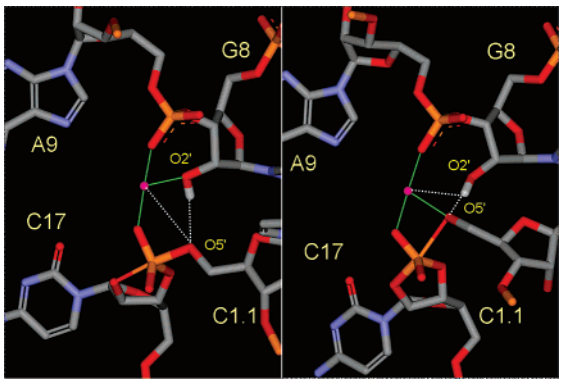

Figure 2. Snapshots of the active site from the early TS mimic (left) and late TS mimic (right) simulations depicting the Mg^{2+} ion direct coordination (green lines) and key hydrogen bonds and indirect Mg^{2+} coordination (dotted lines). For clarity, the water molecules are not shown.

simulation, a transition occurs whereby the Mg^{2+} coordination with the 2′OH of G8 is replaced by direct coordination with the leaving group $O_{5'}$ (Figure 1). In this way, the Mg^{2+} provides electrostatic stabilization of the accumulating charge of the leaving group (i.e., a Lewis acid catalyst).[7] At the same time, the 2′OH of G8 forms a hydrogen bond with the leaving group $O_{5'}$ and is positioned to act as a general acid catalyst (Figure 2, right).

Comparison with Experiment. The present simulation results, together with the crystallographic structure, tie together several key experimental results relating to the role of Mg^{2+} in catalysis. Thio/rescue effect experiments[9] have

suggested that a single metal bound at the P9/G10.1 site (the A9 phosphate in the present work) in the ground state acquires an additional interaction with the scissile phosphate in proceeding to the transition state. Kinetic analysis[30] along with photocross-linking experiments[16] and mutational data[8] have implicated the roles of the 2′OH of G8 and the N_1 of G12 as a general acid and base, respectively, and have been interpreted to be consistent with a transition into an active conformation with appropriate architecture for acid−base catalysis. However, recent kinetic analysis indicates the pK_a of the general acid is downshifted by around 4−7 pK_a units in a metal-dependent manner, correlated with the metal pK_a.[31] The simulation results suggest that the Mg^{2+} interacts strongly with the 2′OH of G8 in the early TS mimic and could contribute to a significant lowering of the pK_a value, and in the late TS mimic the G8 2′OH is hydrogen bonded to the leaving group and poised to act as a general acid catalyst (Figure 2). The Mg^{2+} ion may additionally play a direct role in stabilizing the negative charge accumulated by the leaving group in the late TS, and if a proton from the G8 2′OH is ultimately transferred, the coordination of Mg^{2+} is positioned to revert back to stabilize the resulting G8 2′ alkoxide.

The simulation results presented here are consistent with the direct participation of a single bridging Mg^{2+} ion in hammerhead ribozyme catalysis, although the possibility of involvement of a second ion cannot be definitively precluded.[32,33] The Mg^{2+} preserves the integrity of the active site structure and may serve as an epicenter in the transition state that coordinates the A9 and scissile phosphates, G8 2′OH general acid and $O_{5'}$ leaving group. The present work underscores the need for further investigation of the chemical reaction profile using combined QM/MM models.

ACKNOWLEDGMENT.

The authors are grateful for support from the National Institutes of Health, the IBM-Rochester Life Sciences Group, the Army High Performance Computing Research Center (AHPCRC), and the Minnesota Supercomputing Institute (MSI).

Supporting Information Available: Computational methodology and the rmsd plots of all simulations. This material is available free of charge via the Internet at http://pubs.acs.org.

REFERENCES

(1) Scott, W. G. *Q. Rev. Biophys.* **1999**, *32*, 241−294.
(2) Scott, W. G. *Curr. Opin. Struct. Biol.* **1998**, *8*, 720−726.
(3) Doherty, E. A.; Doudna, J. A. *Annu. Rev. Biophys. Biomol. Struct.* **2001**, *30*, 457−475.
(4) Rubenstein, M.; Tsui, R.; Guinan, P. *Drugs Future* **2004**, *29*, 893−909.
(5) Vaish, N. K.; Dong, F.; Andrews, L.; Schweppe, R. E.; Ahn, N. G.; Blatt, L.; Seiwert, S. D. *Nat. Biotechnol.* **2002**, *20*, 810−815.
(6) Breaker, R. R. *Curr. Opin. Biotechnol.* **2002**, *13*, 31−39.
(7) Takagi, Y.; Ikeda, Y.; Taira, K. *Top. Curr. Chem.* **2004**, *232*, 213−251.
(8) Blount, K. F.; Uhlenbeck, O. C. *Annu. Rev. Biophys. Biomol. Struct.* **2005**, *34*, 415−440.
(9) Wang, S.; Karbstein, K.; Peracchi, A.; Beigelman, L.; Herschlag, D. *Biochemistry* **1999**, *38*, 14363−14378.
(10) Suzumura, K.; Takagi, Y.; Orita, M.; Taira, K. *J. Am. Chem. Soc.* **2004**, *126*, 15504−15511.
(11) Scott, W. G.; Murray, J. B.; Arnold, J. R. P.; Stoddard, B. L.; Klug, A. *Science* **1996**, *274*, 2065−2069.
(12) Murray, J. B.; Terwey, D. P.; Maloney, L.; Karpeisky, A.; Usman, N.; Beigelman, L.; Scott, W. G. *Cell* **1998**, *92*, 665−673.
(13) Murray, J. B.; Szöke, H.; Szöke, A.; Scott, W. G. *Mol. Cell* **2000**, *5*, 279−287.
(14) Martick, M.; Scott, W. G. *Cell* **2006**, *126*, 309−320.
(15) Canny, M. D.; Jucker, F. M.; Kellogg, E.; Khorova, A.; Jayasena, S. D.; Pardi, A. *J. Am. Chem. Soc.* **2004**, *126*, 10848−10849.
(16) Lambert, D.; Heckman, J. E.; Burke, J. M. *Biochemistry* **2006**, *45*, 7140−7147.
(17) Brooks, B. R.; Bruccoleri, R. E.; Olafson, B. D.; States, D. J.; Swaminathan, S.; Karplus, M. *J. Comput. Chem.* **1983**, *4*, 187−217.
(18) Foloppe, N.; MacKerell, A. D., Jr. *J. Comput. Chem.* **2000**, *21*, 86−104.
(19) MacKerell, A. D., Jr.; Banavali, N. K. *J. Comput. Chem.* **2000**, *21*, 105−120.
(20) Mayaan, E.; Moser, A.; Mackerell, A. D., Jr.; York, D. M. *J. Comput. Chem.* In press.
(21) Jorgensen, W. L.; Chandrasekhar, J.; Madura, J. D.; Impey, R. W.; Klein, M. L. *J. Chem. Phys.* **1983**, *79*, 926−935.
(22) Essmann, U.; Perera, L.; Berkowitz, M. L.; Darden, T.; Hsing, L.; Pedersen, L. G. *J. Chem. Phys.* **1995**, *103*, 8577−8593.
(23) Mayaan, E.; Range, K.; York, D. M. *J. Biol. Inorg. Chem.* **2004**, *9*, 807−817.
(24) Peracchi, A.; Beigelman, L.; Scott, E. C.; Uhlenbeck, O. C.; Herschlag, D. *J. Biol. Chem.* **1997**, *272*, 26822−26826.
(25) Peracchi, A.; Beigelman, L.; Usman, N.; Herschlag, D. *Proc. Natl. Acad. Sci. U.S.A.* **1996**, *93*, 11522−11527.
(26) Hermann, T.; Auffinger, P.; Scott, W. G.; Westhof, E. *Nucleic Acids Res.* **1997**, *25*, 3421−3427.
(27) Hermann, T.; Auffinger, P.; Westhof, E. *Eur. Biophys. J.* **1998**, *27*, 153−165.
(28) Torres, R. A.; Bruice, T. C. *Proc. Natl. Acad. Sci. U.S.A.* **1998**, *95*, 11077−11082.
(29) Torres, R. A.; Bruice, T. C. *J. Am. Chem. Soc.* **2000**, *122*, 781−791.
(30) Han, J.; Burke, J. M. *Biochemistry* **2005**, *44*, 7864−7870.
(31) Roychowdhury-Saha, M.; Burke, D. H. *RNA* **2006**, *12*, 1846−1852.
(32) Lott, W. B.; Pontius, B. W.; von Hippel, P. H. *Proc. Natl. Acad. Sci. U.S.A.* **1998**, *95*, 542−547.
(33) Inoue, A.; Takagi, Y.; Taira, K. *Nucleic Acids Res.* **2004**, *32*, 4217−4223.
(34) Leclerc, F.; Karplus, M. *J. Phys. Chem. B* **2006**, *110*, 3395−3409.

CT6003142